High-fidelity quantum gates for trapped ions under micromotion

C. Shen[1,2,*] and L.-M. Duan[1,3]
[1]*Department of Physics, University of Michigan, Ann Arbor, Michigan 48109, USA*
[2]*Department of Applied Physics, Yale University, New Haven, Connecticut 06511, USA*
[3]*Center for Quantum Information, IIIS, Tsinghua University, Beijing 100084, China*
(Received 27 March 2014; revised manuscript received 2 July 2014; published 27 August 2014)

Two- or three-dimensional Paul traps can confine a large number of ions forming a Wigner crystal, which would provide an ideal architecture for scalable quantum computation except for the micromotion, an issue that is commonly believed to be the obstacle for any high-fidelity quantum gate. Here we show that the obstacle of micromotion can be overcome with current technology, even though the magnitude of the micromotion is way outside the Lamb-Dicke region. Through exact solution of the quantum Mathieu equations, we demonstrate the principle of the gate design under micromotion using two ions in a quadrupole Paul trap as an example. The proposed micromotion quantum gates can be extended to the many-ion case and may pave a new way for scalable trapped-ion quantum computation.

DOI: 10.1103/PhysRevA.90.022332 PACS number(s): 03.67.Lx, 03.67.Ac, 37.10.Ty

I. INTRODUCTION

Trapped ions constitute one of the most promising systems for realization of quantum computation. Almost all of the quantum information processing experiments so far have actually been done in linear Paul traps, where the ions form a one-dimensional (1D) crystal along the trap axis [1]. In this configuration, the external rf Paul trap can be well approximated by a static trapping potential, and the micromotion along the trap axis can be neglected, which is believed to be critical for design of high-fidelity quantum gates. However, in terms of scalability, the linear configuration is not the optimal one for realization of large-scale quantum computation: first, the number of ions in a linear trap is limited [2,3]; second and more importantly, the linear configuration is not convenient for realization of fault-tolerant quantum computation. The effective qubit coupling in a large ion chain is dominated by the dipole interaction [4], which is only good for short-range quantum gates because of its fast decay with distance. In a linear chain with short-range quantum gates, the error threshold for fault tolerance is very tough and extremely hard to meet experimentally [5,6].

From a scalability point of view for quantum computation, two- or three-dimensional Paul traps would be much better than a linear chain, where one can hold a large number of qubits with a high error threshold for fault tolerance, in the range of a percent level, even with just the nearest-neighbor quantum gates [6]. Thousands to millions of ions have been successfully trapped to form two- or three-dimensional Wigner crystals in a Paul trap [7]. However, there is a critical problem to using this system for quantum computation, i.e., the micromotion issue. In this high-dimensional configuration, the micromotion cannot be compensated, and the magnitude of the micromotion for each ion can be significantly beyond the optical wavelength (i.e., outside of the Lamb-Dicke regime). As the micromotion is from the driving force of the Paul trap, it cannot be laser cooled. The messy and large-magnitude micromotion well beyond the Lamb-Dicke condition is believed to be a critical hurdle for the design of any quantum gate operation in this architecture. One alternative approach is to construct multizone linear traps and transport ions between different zones [8].

In this paper, we show that the micromotion problem for the design of high-fidelity quantum gates can be overcome with current technology. When the ions form a crystal in a time-dependent Paul trap, they will be described by a set of Mathieu equations. We solve exactly the quantum Mathieu equations with an inhomogeneous driving term and find that the micromotion is dominated by a well-defined classical trajectory with no quantum fluctuation. This large classical motion is significantly outside of the Lamb-Dicke regime; however, it does not lead to infidelity of quantum gates if it is appropriately taken into account in the gate design. The quantum part of the Mathieu equation is described by the secular mode with micromotion correction to its mode function. This part of the motion still satisfies the Lamb-Dicke condition at the Doppler temperature, which is routine for experiments. We use two ions in a quadrupole trap, which has a lot of micromotion, as an example to show the principle of the gate design and give the explicit gate scheme in both the slow and the fast gate regions using multisegment laser pulses [9,10], with the intrinsic gate infidelity arbitrarily approaching zero under large micromotion. We discuss the general procedure of the gate design under micromotion, which can work for any number of ions, with an important implication for large-scale quantum computation.

II. TWO IONS IN A QUADRUPOLE TRAP

To illustrate the general feature of micromotion in Paul traps and the principle of the gate design under micromotion, we consider a three-dimensional (3D) anisotropic quadrupole trap with a time-dependent potential $\Phi(x,y,z) = [U_0 + V_0\cos(\Omega_T t)](\frac{x^2+y^2-2z^2}{d_0^2}) \equiv \alpha(t)(x^2+y^2-2z^2)$ from an electric field oscillating at the rf Ω_T, where U_0, V_0 are voltages for the dc and ac components and d_0 characterizes the size of the trap. We choose a positive U_0 to reduce the effective trap strength along the z direction so that the two ions align

*Corresponding author: chao.shen@yale.edu

along the z axis. Since the motions in different directions do not couple to each other under quadratic expansion, we focus our attention on the z direction. The total potential energy of two ions (each with charge e and mass m) is

$$V(z_1, z_2) = -2e\alpha(t)\left(z_1^2 + z_2^2\right) + \frac{e^2}{4\pi\epsilon_0 |z_1 - z_2|}. \quad (1)$$

We define the center-of-mass (c.m.) coordinate $u_{\text{c.m.}} = (z_1 + z_2)/2$ and the relative coordinate $u_r = z_1 - z_2$. Without loss of generality, we assume $u_r > 0$ and its average $\bar{u}_r = u_0$. We assume the magnitude of the ion motion is significantly less than the ion separation, which is always true for the ions in a crystal phase. The Coulomb interaction can then be expanded around the average distance $\bar{u}_r$ up to the second order of $|u_r - u_0|$. Under this expansion, the total Hamiltonian $H = p_{\text{c.m.}}^2/4m + p_r^2/m + V(z_1, z_2)$ is quadratic (although time dependent) in terms of the coordinate operators $u_{\text{c.m.}}$,u_r and the corresponding momentum operators $p_{\text{c.m.}} = p_1 + p_2$, $p_r = (p_1 - p_2)/2$. The Heisenberg equations under this Hamiltonian H yield the following quantum Mathieu equations for the coordinate operators $u_{\text{c.m.}}$ and u_r:

$$\frac{d^2 u_{\text{c.m.}}}{d\xi^2} + [a_{\text{c.m.}} - 2q_{\text{c.m.}} \cos(2\xi)]u_{\text{c.m.}} = 0, \quad (2)$$

$$\frac{d^2 u_r}{d\xi^2} + [a_r - 2q_r \cos(2\xi)]u_r = f_0, \quad (3)$$

where the dimensionless parameters $a_{\text{c.m.}} = -16eU_0/(md_0^2\Omega_T^2)$, $a_r = a_{\text{c.m.}} + 4e^2/(\pi\epsilon_0 m u_0^3 \Omega_T^2)$, $q_{\text{c.m.}} = q_r = 8eV_0/(md_0^2\Omega_T^2)$, and the dimensionless time $\xi = \Omega_T t/2$. The driving term $f_0 = 6e^2/(\pi\epsilon_0 m u_0^2 \Omega_T^2)$. The quantum operators $u_{\text{c.m.}}$ and u_r satisfy the same form of the Mathieu equations (except for the driving term f_0) as the classical variables. As these equations are linear, we can use the solutions known for the classical Mathieu equation to construct a quantum solution that takes into account the quantum fluctuation.

It is well known that the solution to the classical Mathieu equation $\frac{d^2}{d\xi^2}v + [a - 2q\cos(2\xi)]v = 0$ is a combination of Mathieu sine $S(a, q, \xi)$ and Mathieu cosine $C(a, q, \xi)$ functions, which reduce to the conventional sine and cosine functions when micromotion is neglected [11]. The solution to a homogeneous quantum Mathieu equation $\frac{d^2}{d\xi^2}\hat{u} + [a - 2q\cos(2\xi)]\hat{u} = 0$ can be described using the reference oscillator technique [12]. From the classical solution v and the quantum operator $\hat{u}$, one can introduce the following annihilation operator of a reference oscillator (remember that $\xi = \Omega_T t/2$ is the dimensionless time):

$$\hat{a}(t) = \sqrt{\frac{m}{2\hbar\omega}} i[v(t)\dot{\hat{u}}(t) - \dot{v}(t)\hat{u}(t)], \quad (4)$$

where ω is a normalization constant typically taken as the secular motion frequency of the corresponding Mathieu equation. In addition, we impose the initial condition for $v(t)$ with $v(t)|_{t=0} = 1$ and $\dot{v}(t)|_{t=0} = i\omega$. The position operator $\hat{u}(t)$ and its conjugate momentum $\hat{p}(t) \equiv m\dot{\hat{u}}(t)$ satisfy the commutator $[\hat{u}(t), \hat{p}(t)] = i\hbar$. From the above definition, one can easily check that $\frac{d}{dt}\hat{a}(t) \propto v\frac{d^2}{d\xi^2}\hat{u} - \hat{u}\frac{d^2}{d\xi^2}v = 0$, so $\hat{a}(t) \equiv \hat{a}$ is a constant of motion. Furthermore, $\hat{a}$ and $\hat{a}^\dagger$ satisfy the standard commutator

$$[\hat{a}, \hat{a}^\dagger] = (m/2\hbar\omega)(i\hbar/m)[v(t)\dot{v}^*(t) - v^*(t)\dot{v}(t)]|_{t=0} = 1.$$

When micromotion is neglected, $v(t) = e^{i\omega t}$, and $\hat{a}$ reduces to the annihilation operator of a harmonic oscillator. In the presence of micromotion, $v(t) = C(a, q, \xi) + iS(a, q, \xi)$. The solution to the position operator $\hat{u}$ takes the form

$$\hat{u}(t) = u_0[v^*(t)\hat{a} + v(t)\hat{a}^\dagger], \quad (5)$$

where $u_0 \equiv \sqrt{\hbar/2m\omega}$ is the oscillator length.

The above solution gives a complete description of the center-of-mass motion with the operator

$$u_{\text{c.m.}}(t) = u_{0\text{c.m.}}[v_{\text{c.m.}}^*(t)\hat{a}_{\text{c.m.}} + v_{\text{c.m.}}(t)\hat{a}_{\text{c.m.}}^\dagger], \quad (6)$$

where $u_{0\text{c.m.}} \equiv \sqrt{\hbar/4m\omega_{\text{c.m.}}}$ and $\omega_{\text{c.m.}}$ is the secular frequency of the center-of-mass mode. The relative motion u_r satisfies the inhomogeneous quantum Mathieu equation (3). To solve it, we let $u_r = u_r' + \bar{u}_r$, where u_r' is an operator that inherits the commutators for u_r and satisfies the homogenous quantum Mathieu equation and $\bar{u}_r$ is a classical variable corresponding to a special solution of the Mathieu equation, $\frac{d^2\bar{u}_r}{d\xi^2} + [a_r - 2q_r\cos(2\xi)]\bar{u}_r = f_0$. The special solution $\bar{u}_r$ can be found through the series expansion $\bar{u}_r = f_0\sum_{n=0}^{+\infty} c_n\cos(2n\xi)$, where the expansion coefficients c_n satisfy the recursion relations $a_r c_0 - q_r c_1 = 1$ and $c_n = D_n(c_{n-1} + c_{n+1} + c_0\delta_{n,1})$ for $n \geqslant 1$ with $D_n \equiv -q_r/(4n^2 - a_r)$. When $a_r \ll 1$ and $q_r \ll 1$, which is typically true under real experimental configurations, c_n rapidly decays to zero, with $|c_{n+1}/c_n| \approx q_r/4(n+1)^2$, and we can keep only the first few terms in the expansion and obtain an analytical expression for $\bar{u}_r$ (see the Appendix). The complete solution of u_r is therefore given by

$$u_r(t) = u_{0\text{r}}[v_r^*(t)\hat{a}_r + v_r(t)\hat{a}_r^\dagger] + \bar{u}_r(t), \quad (7)$$

where $u_{0\text{r}} \equiv \sqrt{\hbar/m\omega_r}$ and ω_r is the secular frequency of the relative mode.

III. HIGH-FIDELITY GATE DESIGN

Now we show how to design high-fidelity quantum gates under micromotion. To perform the controlled-phase-flip (CPF) gate [13], we apply laser-induced spin-dependent force on the ions, with the interaction Hamiltonian described by [10]

$$H = \sum_{j=1}^{2} \hbar\Omega_j \cos(\Delta k_z z_j + \delta t + \phi_j)\sigma_j^z, \quad (8)$$

where Δk_z is the wave-vector difference of the two Raman beams along the z direction, δ is the two-photon Raman detuning, Ω_j (real) is the Raman Rabi frequency for ion j, and ϕ_j is the corresponding initial phase. In terms of the normal modes, the position operator $z_j = u_{\text{c.m.}} - (-1)^j u_r/2$, where $u_{\text{c.m.}}, u_r$ are given by Eqs. (6) and (7). We introduce three Lamb-Dicke parameters, $\eta_{\text{c.m.}} \equiv \Delta k_z u_0^{\text{c.m.}}$ for the c.m. mode, $\eta_{\text{r}} \equiv \Delta k_z u_0^{\text{r}}/2$ for the relative mode, and $\eta_{\text{mm}} \equiv \Delta k_z \bar{u}_r/2$ for pure micromotion. Under typical experimental configurations, $\eta_{\text{c.m.}} \sim \eta_r \ll 1$. The parameter η_{mm} is a classical variable that oscillates rapidly with time by multiples of the micromotion frequency Ω_T. In Fig. 1(a), we show a typical trajectory of $\eta_{\text{mm}}(t)$. The magnitude of variation of η_{mm} is considerably larger than 1. In Fig. 1(b), we also plot the function $v_{\text{c.m.}}(t)$,

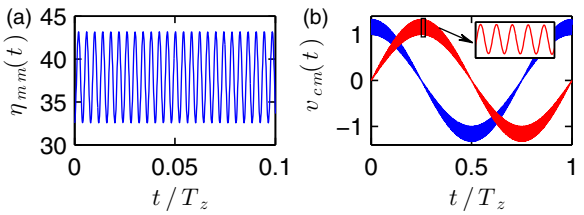

FIG. 1. (Color online) (a) The time-dependent parameter $\eta_{mm}(t)$ and (b) the real and imaginary parts of function $v_{\text{c.m.}}(t)$. The blue (dark gray) curve with starting value near 1 is the real part, and the red (light gray) curve starting from 0 is the imaginary part. They have even and odd parities as a function of time and look similar to cosine and sine functions. Units of time is the trap frequency $T_z = 2\pi/\omega_{\text{c.m.}}$. The parameters used are ion mass $m = 9u$ (u is the atomic mass unit), rf trap frequency $\Omega_T = 2\pi \times 240$ MHz, and characteristic electrode size $d_0 = 200$ μm; the ac and dc voltages V_0 and U_0 are 300 and 21 V, respectively. The resulting secular trap frequencies are $\omega_{\text{c.m.}} = 2\pi \times 0.965$ MHz , $\omega_r = 2\pi \times 3.62$ MHz along the z axis and $\omega_x = \omega_y = 2\pi \times 20.8$ MHz along the x and y axes.

which is dominated by the oscillation at the secular motion frequency $\omega_{\text{c.m.}}$ with a small correction from the micromotion. The magnitude of $v_{\text{c.m.}}(t)$ is bounded by a constant slightly larger than 1. The function $v_r(t)$ has very similar behavior, except that $\omega_{\text{c.m.}}$ is replaced by ω_r. From this consideration of parameters, we can expand the term $\cos(\Delta k_z z_j + \mu t + \phi_j)$ with small parameters $\eta_{\text{c.m.}}, \eta_r$, but η_{mm} is a big term which needs to be treated exactly. After the expansion, to leading order in $\eta_{\text{c.m.}}$ and η_r, the Hamiltonian H takes the form

$$H \approx -\left[\chi_1(t)\sigma_1^z + \chi_2(t)\sigma_2^z\right]\hat{f}_{\text{c.m.}} - \left[\chi_1(t)\sigma_1^z - \chi_2(t)\sigma_2^z\right]\hat{f}_r, \tag{9}$$

where we have defined

$$\begin{aligned} \hat{f}_\mu &\equiv \eta_\mu[v_\mu^*(t)\hat{a}_\mu + v_\mu(t)\hat{a}_\mu^\dagger], \\ \chi_j(t) &\equiv \hbar\Omega_j \sin[\delta t + \phi_j - (-1)^j \eta_{\text{mm}}(t)], \end{aligned} \tag{10}$$

where the subscript $\mu = $ c.m. or r and $j = 1, 2$. In Eq. (9), we have dropped the term $\cos(\delta t + \phi_j \pm \eta_{\text{mm}})$, which induces a single-bit phase shift but is irrelevant for the CPF gate. The evolution operator at the gate time τ generated by the Hamiltonian H can be expressed as

$$U(\tau) = D_{\text{c.m.}}(\alpha_{\text{c.m.}})D_r(\alpha_r)\exp\left[i(\gamma_r - \gamma_{\text{c.m.}})\sigma_1^z\sigma_2^z\right], \tag{11}$$

where the displacement operator $D_\mu(\alpha_\mu) \equiv \exp(\alpha_\mu\hat{a}_\mu^\dagger - \alpha_\mu^*\hat{a}_\mu)$ ($\mu = $ c.m. or r). Let $j_\mu = 1$ for $\mu = $ c.m. and $j_\mu = -1$ for $\mu = $ r. The displacement α_μ and the accumulated phase γ_μ have the following expression:

$$\begin{aligned} \alpha_\mu &= i\eta_\mu \int_0^\tau \left[\chi_1(t)\sigma_1^z + j_\mu\chi_2(t)\sigma_2^z\right]u_\mu(t)\,dt, \\ \gamma_\mu &= i(\eta_\mu)^2 \int_0^\tau dt_1 \int_0^{t_1} dt_2 \mathcal{S}[\chi_1\chi_2]\text{Im}[u_\mu(t_1)u_\mu^*(t_2)], \end{aligned} \tag{12}$$

where $\mathcal{S}[\chi_1\chi_2] \equiv \chi_1(t_1)\chi_2(t_2) + \chi_1(t_2)\chi_2(t_1)$.

To realize the CPF gate, we require $\alpha_\mu = 0$ and $\gamma_r - \gamma_{\text{c.m.}} = \pi/4$. The integrals α_μ can be evaluated semianalytically (see the Appendix) or purely numerically. We normally take $\Omega_1 = \Omega_2 \equiv \Omega$. Note that even in this case $\chi_1(t_1) \neq \chi_2(t_2)$, with the micromotion term $\eta_{\text{mm}}(t)$. This is different from the case of a static trap. From Eq. (12), we see that $\alpha_\mu = 0$ for a fixed μ gives two complex and thus four real constraints. With excitation of N motional modes, the total number of (real) constraints to realize the CPF gate is therefore $4N + 1$ (the condition $\gamma_r - \gamma_{\text{c.m.}} = \pi/4$ gives one constraint). To satisfy these constraints, we divide the Rabi frequency $\Omega(t)$ ($0 \leqslant t \leqslant \tau$) into m equal-time segments and take a constant $\Omega_\beta(\beta = 1, 2, \ldots, m)$ for the βth segment [9,10]. This kind of modulation can be conveniently done through an acoustic optical modulator in experiments [14]. The Rabi frequencies are our control parameters. For the two-ion case, under fixed detuning δ and gate time τ, in general, we can find a solution for the CPF gate with $m = 9$ segments. For some specific detuning δ very close to a secular mode frequency, off-resonant excitations become negligible, and a solution is possible under one segment of the pulse by tuning of the gate time τ, which corresponds to the case of the Mølmer-Sørensen gate [15] generalized to include the micromotion correction.

To characterize the quality of the gate, we use the fidelity $F \equiv \text{tr}_\mu[\rho_\mu|\langle\Psi_0|U_{\text{CPF}}^\dagger U(\tau)|\Psi_0\rangle|^2]$, defined as the overlap of the evolution operator $U(\tau)$ with the perfect one $U_{\text{CPF}} \equiv e^{i\pi\sigma_1^z\sigma_2^z/4}$ under the initial state $|\Psi_0\rangle$ for the ion spins and the thermal state ρ_μ for the phonon modes. In our calculation, without loss of generality, we take $|\Psi_0\rangle = (|0\rangle + |1\rangle) \otimes (|0\rangle + |1\rangle)/2$ and assume the Doppler temperature T_D ($k_B T_D/h \approx 10$ MHz for Be^+ ion) for all the phonon modes. For any given detuning δ and gate time τ, we optimize the control parameters $\Omega_\beta(\beta = 1, 2, \ldots, m)$ to get the maximum fidelity F. In Fig. 2, we show the gate fidelity as a function of gate time for $\delta = 0.95\omega_{\text{c.m.}}$ (close to a secular frequency) by applying a single-segment laser pulse of a constant Rabi frequency Ω. In Fig. 2, the dashed line corresponds to the result in a static harmonic trap with the same secular frequencies but no micromotion. If we take into account the micromotion

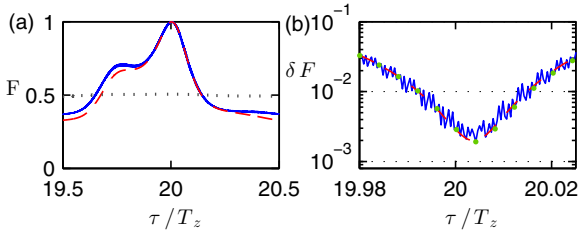

FIG. 2. (Color online) (a) The fidelity of a two-ion conditional phase-flip gate as a function of gate time τ, where the unit of time is the period of the center-of-mass motion along the z direction $T_z = 2\pi/\omega_{\text{c.m.}}$. The detuning was chosen to be $\mu = 0.95\omega_{\text{c.m.}z}$. The blue solid line indicates the optimal results with micromotion taken into account; the red dashed line is the result for a genuine static harmonic trap without micromotion, and the gray dotted line is obtained by applying the optimal solution for a static harmonic trap to the case with micromotion, which results in poor performance. (b) The infidelity (one-fidelity) near the optimal evolution time, essentially a close-up of (a) near $\tau = 20T_z$. The green dots in (b) show the time points that are an integral multiple of the micromotion period. The other parameters used are temperature of both motional degrees of freedom $k_B T = 10\hbar\omega_{\text{c.m.}}$ and effective laser wave vector $\Delta k_z = 8\,\mu\text{m}^{-1}$, so $\eta_{\text{c.m.}} \approx 0.12$ and $\eta_r \approx 0.09$.

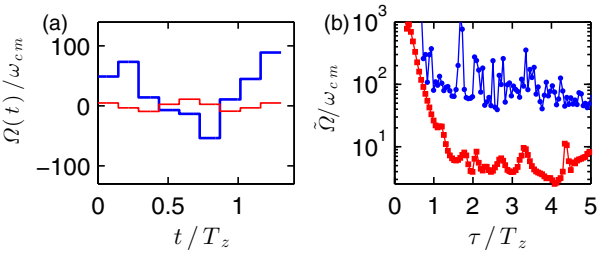

FIG. 3. (Color online) (a) The waveform of the optimal segmented pulse calculated for the gate with duration $\tau = 1.31T_z$. The thick blue (thin red) line corresponds to the case with (without) micromotion. (b) The maximal Rabi frequency $\tilde{\Omega} \equiv \max_t |\Omega(t)|$ as a function of the gate time τ. The upper blue (lower red) curve corresponds to the case with (without) micromotion.

contribution but do not change the gate design, the result is described by the dash-dotted line, with a low fidelity of only about 50%. When we optimize the gate design (optimize Ω_β) including the micromotion correction, the gate fidelity is represented by the solid line, which approaches the optimal fidelity achievable in a static trap. The gate infidelity $\delta F \equiv 1 - F$ approaches 2×10^{-3} at the optimal gate time $\tau = 20.005T_z$, where $T_z \equiv 2\pi/\omega_{\text{c.m.}}$.

By applying nine segments of laser pulses with optimized $\Omega_\beta(\beta = 1,2,\ldots,9)$, the gate fidelity F can attain unity at arbitrary detuning δ for the two-ion case. As an example, in Fig. 3(a), we show the optimized solution of Ω_β (thick blue line) at an arbitrarily chosen detuning $\delta = 1.4\omega_{\text{c.m.}}$. For comparison, the thin red line represents the solution of Ω_β in a static harmonic trap with otherwise the same parameters. The maximum magnitude of $|\Omega_\beta|$ significantly increases in the case of micromotion. This is understandable as fast oscillations of the micromotion tend to lower the effective Rabi frequencies, as confirmed by experiments performed in the presence of micromotion [16,17]. In Fig. 3(b), we show the maximum magnitude of $|\Omega_\beta|$ as a function of the gate time τ. Compared with the solution in a static harmonic trap, the maximum $|\Omega_\beta|$ in general needs to increase by about an order of magnitude under micromotion.

IV. CONCLUSION

In conclusion, we have demonstrated that arbitrarily high fidelity quantum gates can be achieved under significant micromotion. The explicit demonstration in this paper uses the example of two ions in a quadrupole trap, which has a micromotion magnitude significantly beyond the Lamb-Dicke limit. Apparently, the idea here is applicable to the many-ion case in higher dimensions [18]. For a system of N ions in any dimension, as long as the ions crystallize, each ion has an average equilibrium position. We can then expand the Coulomb potential around these equilibrium positions. Under the rf Paul trap and the Coulomb interaction, the motion of the ions can then be described by a set of coupled time-dependent Mathieu equations [19]. Using the technique in this paper, we can solve the motional dynamics and optimize the gate design that explicitly takes into account all the micromotion contributions. The gate design technique under micromotion proposed in this paper solves a major obstacle for high-fidelity quantum computation in real rf traps beyond the 1D limitation and opens a way for scalable quantum computation based on large two- or three-dimensional trap-ion crystals in Paul traps.

ACKNOWLEDGMENTS

This work was supported by the NBRPC (973 Program), Grant No. 2011CBA00300 (2011CBA00302), the IARPA MUSIQC program, the ARO and the AFOSR MURI programs, and the DARPA OLE program.

APPENDIX

In this appendix, we show in detail how to solve the driven Mathieu equation and give an approximate treatment of the motional integrals.

1. Solution of the driven mathieu equation

We show in detail how to solve the Mathieu equation with a constant drive term.

$$\frac{d^2u}{d\xi^2} + [a - 2q\cos(2\xi)]u = f_0.$$

Let us assume that $u(\xi) = f_0 \sum_{n=0}^{\infty} c_n \cos(2n\xi)$ and insert it into the equation. After re-organization, we get

$$ac_0 - qc_1 + \sum_{n=1}^{\infty}[(a - 4n^2)c_n - q(c_{n-1} + c_{n+1}) - qc_0\delta_{n,1}] \times \cos(2nt) = 1.$$

Defining $D_n \equiv (a - 4n^2)/q$, we have the following set of linear equations:

$$ac_0 - qc_1 = 1, \quad c_n - \frac{1}{D_n}(c_{n-1} + c_{n+1} + c_0\delta_{n,1}) = 0.$$

In matrix form,

$$\begin{pmatrix} a & -q & 0 & \cdots & & 0 \\ -\frac{2}{D_1} & 1 & -\frac{1}{D_1} & & & \\ 0 & -\frac{1}{D_2} & 1 & -\frac{1}{D_2} & & \\ \vdots & & -\frac{1}{D_3} & 1 & -\frac{1}{D_3} & \\ & & & \ddots & \ddots & \\ 0 & & & & & \end{pmatrix} \cdot \begin{pmatrix} c_0 \\ c_1 \\ c_2 \\ \vdots \end{pmatrix} = \begin{pmatrix} 1 \\ 0 \\ 0 \\ \vdots \end{pmatrix}. \tag{A1}$$

The factor $1/D_n$ decreases very fast as n increases, and we can truncate the expansion of $u(\xi)$ at a small n. Numerically, we observe that, typically, keeping up to c_2 already gives enough accuracy. We can thus get a very accurate analytical expression:

$$c_0 \approx \frac{64 + a(a-20) - q^2}{(32-3a)q^2 + a(a-4)(a-16)},$$

$$c_1 \approx \frac{2(a-16)q}{(32-3a)q^2 + a(a-4)(a-16)},$$

$$c_2 \approx \frac{2q^2}{(32-3a)q^2 + a(a-4)(a-16)}.$$

For the example in the main text, $a_r = -0.0388$ and $q_r = 0.283$, we have $c_0 = 1132.8$ and $u_r(\xi) = f_0 c_0[1 - 0.14\cos(2\xi) + 0.0025\cos(4\xi) + \dots]$.

The micromotion-corrected equilibrium position is $f_0 c_0$ and should be identified with u_0, around which we expand the Coulomb potential in the first place. Thus we should determine them self-consistently. Taking the relative motion in the paper as an example, since both $a| \equiv \frac{-16eU_0}{md_0^2\Omega_T^2} + \frac{4e^2}{\pi\epsilon_0 m u_o^3 \Omega_T^2}$ and $f_0 \equiv \frac{6e^2}{\pi\epsilon_0 m u_0^2 \Omega_T^2}$ are functions of u_0, then the self-consistent equation

$$u_0 = f_0 c_0 \approx f_0 \frac{64 + a_r(a_r - 20) - q_r^2}{(32 - 3a_r)q_r^2 + a_r(a_r - 4)(a_r - 16)}$$

gives the correct u_0. With the iterative method it typically takes only a few iterations to converge to the correct value when starting from a proper initial value of u_0.

2. Two-stage time integral

Here we offer an approximate treatment of motional integrals. We notice that the secular frequency ω and the micromotion frequency Ω are well separated, i.e., $\omega \ll \Omega$. This means quantities with the characteristic frequency ω or less stay constant within one period of micromotion. So we can perform the time integral in two steps: we first integrate over one period of the micromotion, obtaining a slowly varying integrand, which we then integrate again. By doing this we will show that the dominant effect of micromotion is to modulate the effective Rabi frequency. Notice that the integrals $\int_0^\tau \chi(t)u(t)\,dt$ can be reduced to the form (ignoring micromotion frequencies $n\Omega \pm \omega$ with $n \geqslant 2$)

$$I = \int_0^\tau dt\, \sin\{a_0(t) + a_1(t)\cos[\Omega t_1 + \phi(t)]\} \times \{b_0(t) + b_1(t)\cos[\Omega t + \varphi(t)]\},$$

where $a_0(t)$, $a_1(t)$, $b_0(t)$, $b_1(t)$, $\phi(t)$, and $\varphi(t)$ are all real slowly varying functions within one period of micromotion $\frac{2\pi}{\Omega}$. The above integral can be further broken into two parts, I_1 and I_2, where

$$\begin{aligned} I_1 &\approx \int_0^\tau dt \frac{\Omega}{2\pi} \int_t^{t+2\pi/\Omega} dt_1\, \sin[a_0(t) + a_1(t)\cos(\Omega t_1 + \phi)]b_0(t) \\ &= \int_0^\tau dt\, \frac{1}{2\pi} \int_{-\pi}^{\pi} dt'\, \sin[a_0(t) + a_1(t)\cos(t')]b_0(t) \\ &= \mathrm{Im}\left[\int_0^\tau dt\, \exp[i\, a_0(t)]\frac{1}{2\pi}\int_{-\pi}^{\pi} dt'\, \exp[i\, a_1\cos(t')]b_0(t)\right] \\ &\quad \times \mathrm{Im}\left[\int_0^\tau dt\, \exp[i\, a_0(t)]J_0(a_1)b_0(t)\right] \\ &= \int_0^\tau dt\, \sin[a_0(t)]b_0(t)J_0(a_1(t)) \end{aligned}$$

and

$$\begin{aligned} I_2 &= \int_0^\tau dt\, \sin[a_0(t) + a_1(t)\cos(\Omega t + \phi)]b_1(t)\cos[\Omega t + \varphi(t)] \\ &\approx \int_0^\tau dt \frac{\Omega}{2\pi} \int_t^{t+2\pi/\Omega} dt_1\, \sin[a_0(t) + a_1(t)\cos(\Omega t_1 + \phi)] \\ &\quad \times b_1(t)\cos(\Omega t_1 + \varphi) \\ &= \int_0^\tau dt\, \cos[a_0(t)]\cos(\varphi - \phi)J_1(a_1(t)) \end{aligned}$$

where J_0 and J_1 denote the Bessel functions. In both cases, the micromotion gives rise to slowly varying modulation factors, and $\cos(\varphi - \phi)J_1(a_1(t))$. Moreover in I_2 the phase of the original integrand is also shifted, $\sin[a_0(t)] \to \cos[a_0(t)]$. For the actual experimental system, the term I_2 contributes much less than I_1 to the target integral I because it has a much smaller coefficient for the micromotion component than that of the secular component in $v(t)$. So, in leading order, micromotion reduces the laser Rabi frequency seen by the ion by a factor on the order of $J_0(a_1(t))$.

[1] R. Islam, C. Senko, W. C. Campbell, S. Korenblit, J. Smith, A. Lee, E. E. Edwards, C.-C. J. Wang, J. K. Freericks, and C. Monroe, Science **340**, 583 (2013); H. Häffner *et al.*, Nature (London) **438**, 643 (2005); C. A. Sackett *et al.*, *ibid.* **404**, 256 (2000); F. Schmidt-Kaler, H. Häffner, M. Riebe, S. Gulde, G. P. T. Lancaster, T. Deuschle, C. Becher, C. F. Roos, J. Eschner, and R. Blatt, *ibid.* **422**, 408 (2003); J. Benhelm, G. Kirchmair, C. F. Roos, and R. Blatt, Nat. Phys. **4**, 463 (2008); K. Kim, M.-S. Chang, S. Korenblit, R. Islam, E. E. Edwards, J. K. Freericks, G.-D. Lin, L.-M. Duan, and C. Monroe, Nature (London) **465**, 590 (2010); R. Islam *et al.*, Nat. Commun. **2**, 377 (2011); B. P. Lanyon *et al.*, Science **334**, 57 (2011); B. P. Lanyon, P. Jurcevic, M. Zwerger, C. Hempel, E. A. Martinez, W. Dur, H. J. Briegel, R. Blatt, and C. F. Roos, Phys. Rev. Lett. **111**, 210501 (2013).

[2] M. G. Raizen, J. M. Gilligan, J. C. Bergquist, W. M. Itano, and D. J. Wineland, Phys. Rev. A **45**, 6493 (1992).

[3] J. P. Schiffer, Phys. Rev. Lett. **70**, 818 (1993).

[4] Although the ion-ion Coulomb interaction is the $1/r$ type, this interaction is spin (qubit) independent. The effective qubit interaction comes from the second-order gradient of the $1/r$ potential under a spin-dependent force on both qubits and thus scales as $1/r^3$.

[5] D. Gottesman, J. Mod. Opt. **47**, 333 (2000); K. M. Svore, B. M. Terhal, and D. P. DiVincenzo, Phys. Rev. A **72**, 022317 (2005); T. Szkopek, P. O. Boykin, H. Fan, V. P. Roychowdhury, E. Yablonovitch, G. Simms, M. Gyure, and B. Fong, IEEE Trans. Nanotechnol. **5**, 42 (2006).

[6] R. Raussendorf and J. Harrington, Phys. Rev. Lett. **98**, 190504 (2007); D. S. Wang, A. G. Fowler, C. D. Hill, and L. C. L. Hollenberg, Quantum Inf. Comput. **10**, 780 (2010).

[7] A. Mortensen, E. Nielsen, T. Matthey, and M. Drewsen, Phys. Rev. Lett. **96**, 103001 (2006); K. Okada, T. Takayanagi, M. Wada, S. Ohtani, and H. A. Schuessler, Phys. Rev. A **80**, 043405 (2009); B. Szymanski, R. Dubessy, B. Dubost, S. Guibal, J.-P. Likforman, and L. Guidoni, Appl. Phys. Lett. **100**, 171110 (2012); M. Drewsen, T. Matthey, A. Mortensen, and J. P. Hansen, arXiv:1202.2544.

[8] D. Kielpinski, C. Monroe, and D. J. Wineland, Nature (London) **417**, 709 (2002).

[9] S.-L. Zhu, C. Monroe, and L.-M. Duan, Europhys. Lett. **73**, 485 (2006).

[10] S.-L. Zhu, C. Monroe, and L.-M. Duan, Phys. Rev. Lett. **97**, 050505 (2006).

[11] N. W. McLachlan, *Theory and Application of Mathieu Functions* (Clarendon, Oxford, 1947).

[12] M. Combescure, Ann. Inst. Henri Poincare, Sect. A **44**, 293 (1986); L. S. Brown, Phys. Rev. Lett. **66**, 527 (1991); R. J. Glauber, in *Laser Manipulation of Atoms and Ions: Proceedings of the International Enrico Fermi School, Course 118, Varenna, Italy, July 1–19, 1992*, edited by E. Arimondo, W. D. Phillips, and F. Strumia (North Holland, Amsterdam, 1992), pp. 643–660; B. E. King, Ph.D. thesis, University of Colorado at Boulder, 1999.

[13] Direct implementation of other entangling gates is also possible, such as the gates required in M.-H. Yung *et al.* [Sci. Rep. **4**, 3589 (2014)], although the CPF gate is already universal together with single-bit operations.

[14] T. Choi, S. Debnath, T. A. Manning, C. Figgatt, Z.-X. Gong, L.-M. Duan, and C. Monroe, Phys. Rev. Lett. **112**, 190502 (2014).

[15] A. Sørensen and K. Mølmer, Phys. Rev. Lett. **82**, 1971 (1999).

[16] Q. A. Turchette, C. S. Wood, B. E. King, C. J. Myatt, D. Leibfried, W. M. Itano, C. Monroe, and D. J. Wineland, Phys. Rev. Lett. **81**, 3631 (1998).

[17] H. Kaufmann, S. Ulm, G. Jacob, U. Poschinger, H. Landa, A. Retzker, M. B. Plenio, and F. Schmidt-Kaler, Phys. Rev. Lett. **109**, 263003 (2012).

[18] S.-T. Wang, C. Shen, and L.-M. Duan (unpublished).

[19] see H. Landa, M. Drewsen, B. Reznik, and A. Retzker, New J. Phys. **14**, 093023 (2012); J. Phys. A **45**, 455305 (2012).